LBNL-40942
UC-401
Preprint

ERNEST ORLANDO LAWRENCE
BERKELEY NATIONAL LABORATORY

Photodissociation of Acrylonitrile at 193 nm: A Photofragment Translational Spectroscopy Study Using Synchrotron Radiation for Product Photoionization

David A. Blank, Arthur G. Suits, Yuan T. Lee,
Simon W. North, and Gregory E. Hall

Chemical Sciences Division

October 1997

Submitted to
Journal of Chemical Physics

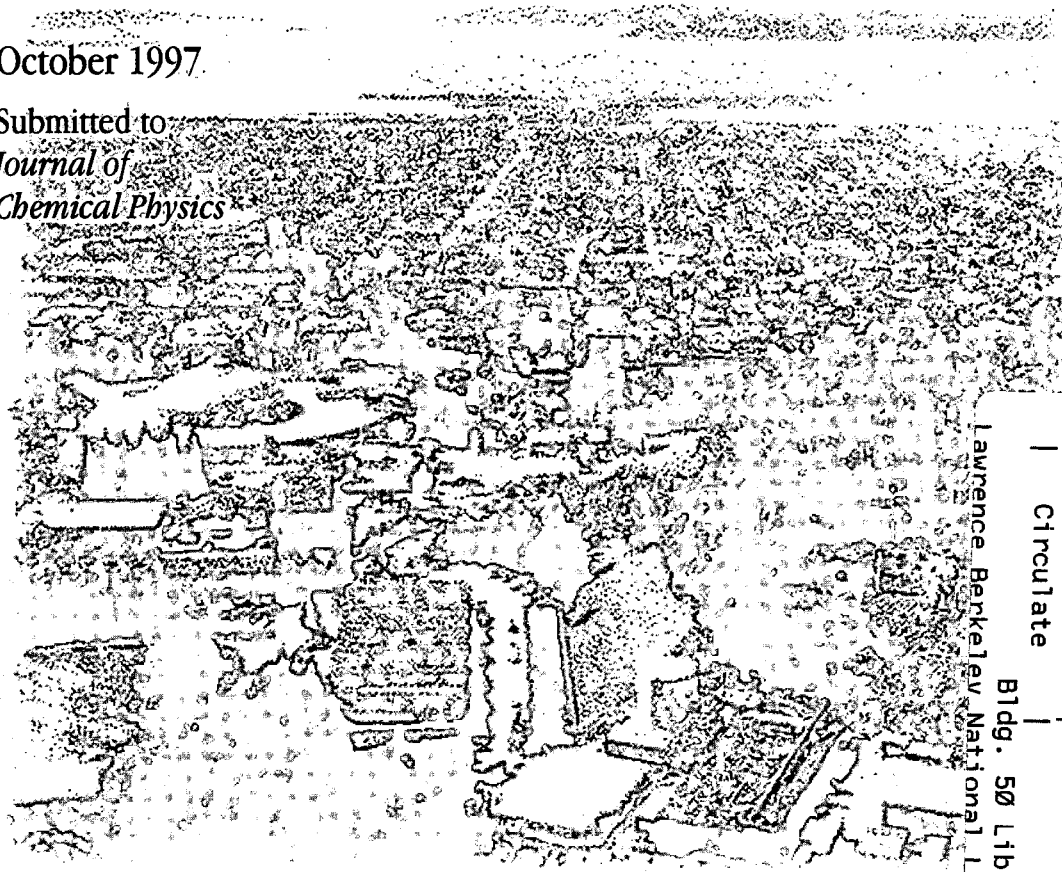

DISCLAIMER

LBNL-40942
UC-401

Photodissociation of Acrylonitrile at 193 nm: A Photofragment Translational Spectroscopy Study Using Synchrotron Radiation for Product Photoionization

David A. Blank, Arthur G. Suits, and Yuan T. Lee

Chemical Sciences Division
Ernest Orlando Lawrence Berkeley National Laboratory
University of California
Berkeley, California 94720

Simon W. North and Gregory E. Hall

Chemistry Department
Brookhaven National Laboratory
Upton, New York 11973-5000

October 1997

This work was supported by the Director, Office of Energy Research, Office of Basic Energy Sciences, Chemical Sciences Division, of the U.S. Department of Energy under Contract No. DE-AC03-76SF00098. Support was also given by the Brookhaven National Laboratory under Contract No. DE-AC02-76CH00016.

Photodissociation of acrylonitrile at 193 nm: a photofragment translational spectroscopy study using synchrotron radiation for product photoionization

David A. Blank, Arthur G. Suits, and Yuan T. Lee
Chemical Sciences Division, Lawrence Berkeley Laboratory, University of California, and Chemistry Department, University of California, Berkeley, CA, 94720

Simon W. North[a] and Gregory E. Hall
Chemistry Department, Brookhaven National Laboratory, Upton, NY, 11973-5000

Abstract

We have investigated the photodissociation of acrylonitrile (H_2CCHCN) at 193 nm using the technique of photofragment translational spectroscopy. The experiments were performed at the Chemical Dynamics Beamline at the Advanced Light Source and used tunable vacuum ultraviolet synchrotron radiation for product photoionization. We have identified four primary dissociation channels including atomic and molecular hydrogen elimination, HCN elimination, and CN elimination. There is significant evidence that all of the dissociation channels occur on the ground electronic surface following internal conversion from the initially optically prepared state. The product translational energy distributions reflect near statistical simple bond rupture for the radical dissociation channels, while substantial recombination barriers mediate the translational energy release for the two molecular elimination channels. Photoionization onsets have provided additional insight into the chemical identities of the products and their internal energy content.

---

[a] Present address: Department of Chemistry, Texas A&M University, College Station, TX, 77843

1. Introduction

As the simplest π-bonded hydrocarbons, ethylene and its substituted analogues serve as prototypical systems for the study of this important class of molecules. These compounds exhibit a strong $\pi^* \leftarrow \pi$ transition around 190 nm and their photochemistry following excitation has been the subject of considerable literature. At excitation wavelengths <200 nm there is sufficient available energy for both radical (rxn 1 and 2) and molecular (rxn 3 and 4) elimination channels.

$$H_2CCHX \rightarrow C_2H_2X + H \qquad \text{(rxn 1)}$$

$$H_2CCHX \rightarrow C_2H_3 + X \qquad \text{(rxn 2)}$$

$$H_2CCHX \rightarrow C_2HX + H_2 \qquad \text{(rxn 3)}$$

$$H_2CCHX \rightarrow C_2H_2 + HX \qquad \text{(rxn 4)}$$

Understanding the competition between these dissociation pathways as well as the underlying dynamics of each channel has been central to previous experimental investigations.

The photochemistry of ethylene has been the subject of numerous studies.[1] Balko *et al.* used the technique of photofragment translational spectroscopy (PTS) to study the dissociation of ethylene at 193 nm. The authors characterized both the atomic and molecular hydrogen elimination channels which were found to occur with nearly equal yields. Both dissociation channels followed internal conversion (IC) to the ground electronic surface. The hydrogen atom loss channel exhibited a center of mass (c.m.) translational energy distribution ($P(E_T)$) consistent with statistical bond rupture involving little or no barrier to recombination. The $P(E_T)$ for the molecular hydrogen elimination channel was peaked at 20 kcal/mol reflecting a substantial recombination barrier. From the dissociation of selectively deuterated ethylene isotopomers a 2:3 ratio of 1,1 versus 1,2 H_2 elimination was determined. Based on thermodynamic considerations, the 1,1 elimination

was assigned predominantly to the production of singlet vinylidene, contrary to previous reports.[2] In addition, the authors also measured the $P(E_T)$ for hydrogen atoms which resulted from the subsequent dissociation of the nascent vinyl radical photoproducts.

Of the mono-substituted ethylenes, the photodissociation of vinyl chloride has received the greatest attention.[3] We mention here only a few of the key points from the results of those investigations. Gordon and coworkers have pursued an extensive series of studies investigating the dissociation of vinyl chloride at 193 nm using Doppler spectroscopy. The authors have measured Doppler profiles for hydrogen atom products with an average translational energy of 17 kcal/mol assuming a Maxwell-Boltzmann distribution. They also measured the rotational distributions for H_2 (v=0-4) products and obtained the maximum translational energy release for several states of H_2 from the measured Doppler profiles. The focus of these investigations has been the Cl and HCl elimination channels. The bimodal translational energy distribution for the radical Cl elimination channel was originally assigned as two dissociation channels based on the results of Umemoto *et al.* for 1,1 dichloroethylene. The faster fragments were thought to originate from the σ^*(C-Cl) electronic surface while the slower fragments originated from a ground state dissociation.[4] The state resolved $P(E_T)$'s for HCl measured by Gordon and coworkers were qualitatively similar to the $P(E_T)$ measured by Balko *et al.* for H_2 elimination from ethylene.[1] The HCl rotational population was found to be biexponential for v=0 and was fit well with a single Boltzmann rotational temperature for v=1 and v=2. Gordon and coworkers also dissociated vinyl chloride-1d at 193 nm and found a 25:75 ratio of HCl:DCl. While this might suggest a 25:75 ratio of 1,2 versus 1,1 HCl elimination, this conclusion was contradicted by the identical internal energy distributions of the HCl and DCl products. A complex mechanism involving partial H-atom scrambling followed by a concerted 1,1 HCl elimination and isomerization of the singlet vinylidene product to acetylene was invoked to explain the experimental results.

The photodissociation of acrylonitrile (H_2CCHCN) has received comparably less attention. The vacuum ultraviolet absorption spectrum was measured by Mullen and

Orloff who assigned the following transitions: $n \rightarrow \pi^*$ at 217.0 nm, $\pi \rightarrow \pi^*$ at 203.0 nm, and $\sigma \rightarrow \sigma^*$ at 172.5 nm.[5] Gandini and Hackett photolyzed acrylonitrile at 213.9 nm and identified end products consistent with the molecular elimination channels, reactions 3 and 4, with a ratio of HCN to H_2 loss of 1.6.[6] The authors noted a drop in the H_2 quantum yield when photolyzing at 206.5 nm and suggested the onset of a competitive radical dissociation channel. Dissociation of acrylonitrile-1d resulted in a ratio of 1.5±0.2 for both HD/H_2 and C_2HD/C_2H_2 and, while the evidence was not conclusive, the authors favored a mechanism where randomization of the H/D atoms precedes elimination of both HCN and H_2. Nishi *et al.* have performed PTS experiments on acrylonitrile at 193 nm.[7] The authors identified two single photon dissociation pathways, CN and HCN elimination. The translational energy distributions for both channels were obtained by a direct inversion of the TOF spectra, and each was fitted with a Boltzmann distribution. The lower energy contribution, T_{bolt}=2500 K, was assigned to the CN elimination channel, and the higher energy contribution, T_{bolt}=6000 K, was assigned to HCN elimination with a ratio of CN/HCN >3. Experiments by Fahr and Laufer employing VUV flash photolysis of acrylonitrile-1d followed by spectroscopic VUV detection of the products suggested that molecular HCN elimination results predominantly from 1,1 elimination on an excited electronic surface to give HCN and *triplet* vinylidene.[8] The authors also placed an upper limit on the CN elimination channel of 5%.

Bird and Donaldson investigated the CN elimination channel at 193 nm using laser-induced fluorescence (LIF) to probe the CN product state distributions.[9] Only v=0 and v=1 vibrational states were populated with a ratio of (v=1/v=0) = 0.14. The nascent rotational distributions for both v=0 and v=1 were fitted with a Boltzmann rotational temperature of T_{bolt}=1450 K. Based on the non-statistical vibrational distribution, the level of rotational excitation, and the translational energy distribution reported by Nishi *et al.* the authors concluded that the CN elimination channel proceeds *via* a prompt dissociation on an excited electronic surface. Recently, North and Hall investigated the CN elimination channel at 193 nm using transient frequency-modulated spectroscopy to measure nascent CN Doppler profiles.[10] The measured CN v=1 to v=0 branching ratio was in good

agreement with the results of Bird and Donaldson. The CN Doppler profiles, however, were consistent with a prior translational energy distribution and showed no detectable vector correlations, suggesting that the dissociation proceeds *via* simple bond rupture on the ground electronic surface. The authors also determined a quantum yield of <0.01 for the CN elimination channel.

We have recently demonstrated the power of the technique of photofragment translational spectroscopy with tunable VUV synchrotron radiation used for product photoionization to resolve a complete picture of complex photodissociation dynamics in small molecular systems.[11] In this study we have used this method to investigate the photodissociation of acrylonitrile at 193 nm. Figure 1 shows the thermodynamically available dissociation channels following absorption at 193 nm. We have identified four primary dissociation channels including both of the radical dissociation channels, reactions 1 and 2, and both of the molecular elimination channels, reactions 3 and 4. The dissociation is consistent with competition on the ground electronic surface following internal conversion from the initially excited $\pi\pi^*$ state. Translational energy distributions have been determined for all of the observed dissociation channels. The selective photoionization has enabled us to distinguish between signals generated by molecular HCN elimination and radical CN elimination, despite the identical product mass combinations (m/e 27 + m/e 26) of these dissociation channels. Additionally, we have measured the photoionization onsets for all of the dissociation products heavier than H_2, providing additional information about their identities and extents of internal excitation.

2. Experimental

These experiments were carried out at the Chemical Dynamics Beamline at the Advanced Light Source (ALS) at Lawrence Berkeley National Laboratory. A complete description of the apparatus can be found in reference 12. The instrument is based on a previously constructed apparatus that is described in detail elsewhere[13] with the most significant difference being the use of tunable VUV undulator radiation from the ALS for

product photoionization in place of electron impact. A continuous molecular beam was generated by expanding 100 Torr of 3% or 11% acrylonitrile in He through a 0.125 mm nozzle into a source chamber maintained at $4x10^{-4}$ Torr. The nozzle was heated to ~200 °C to inhibit cluster formation. The velocity distribution of the resulting beam was measured by chopping the beam with a slotted mechanical wheel. The beam velocity for 3% acrylonitrile in He was 1710 m/s with a FWHM of 12% and for 11% acrylonitrile in He was 1330 m/s with a FWHM of 13%. The molecular beam was skimmed twice and intersected at 90° with the output of a Lambda Physik LPX-200 excimer laser operating on the ArF transition (193.3 nm). Laser fluence ranged 10-300 mJ/cm^2. The molecular beam was rotatable about the axis of the photodissociation laser. Neutral photodissociation products which recoiled out of the molecular beam traveled 15.1 cm where they were intersected by VUV undulator radiation and photoionized, mass selected, and counted as a function of time.[14]

The VUV undulator radiation used for product photoionization is described in detail elsewhere.[15] The undulator radiation is continuously tunable from 7-50 eV, has an approximate Gaussian energy distribution with a FWHM of 2.5%, and provides ~$1x10^{16}$ photons/sec at the fundamental energy with substantial energy in the higher harmonics. In order to suppress the higher order harmonics the undulator radiation is focused into a filter consisting of 30 torr of argon.[16] Below the ionization potential (IP) for argon, 15.76 eV[17], the filter is transparent. Above the argon IP, the filter becomes opaque, providing $>10^4$ suppression of the undulator radiation. In addition, there is also a removable MgF_2 window between the rare gas filter and the point of intersection with the photodissociation products. This window can be used at ionization energies below the MgF_2 cutoff of 11.2 eV[18] to provide additional suppression of higher energy radiation. After passing through the rare gas filter, the undulator radiation is refocussed to 150μm x 250μm at the point of intersection with the scattered neutral photodissociation products. The undulator flux is continuously monitored using a VUV calorimeter. For measurements of the photoionization onsets of photodissociation products the total scattering signal at a fixed source angle is integrated as the undulator energy is stepped. For these measurements the

apertures defining the undulator radiation were adjusted to accept less of the radiation cone, narrowing the energy distribution to a FWHM of 2.0% with a 75% reduction in flux.

Acrylonitrile, 99+%, was obtained from Aldrich and used without further purification.

3. Results

Center of mass translational energy distributions, $P(E_T)$, were obtained from the time of flight spectra, TOF, using the forward convolution technique.[19] The forward convolution technique involves convolution of an initial $P(E_T)$ and photofragment angular distribution, $T(\theta)$, over the instrument response function to generate a simulated TOF spectrum. The simulated TOF spectrum is then compared to the experimental data and the $P(E_T)$ and $T(\theta)$ are iteratively adjusted until a best fit to the data is obtained. For all of the TOF spectra presented, the circles represent the data, the dashed lines represent contributions of individual dissociation channels to the forward convolution fit, and the solid line is the total forward convolution fit to the data. While TOF spectra were taken at multiple laser fluences to insure that dissociation signals were the result of a single photon absorption, all TOF spectra presented were taken with a laser fluence of ~100 mJ/cm^2. In all of the experiments presented the photodissociation laser was unpolarized, which has the experimental result of an isotropic laboratory photofragment distribution in the plane defined by the molecular beam and detector.

Hydrogen atom elimination. Figure 2 shows the TOF spectra for m/e 52 ($C_3H_2N^+$) at source angles of 5° and 7.5° and a photoionization energy of 14.0 eV. The spectra contain a single feature which was fitted with the $P(E_T)$ shown as the solid line in Fig. 3. TOF data at m/e 52 could not be collected at scattering angles less than 5 degrees due to background from the molecular beam. A minimum of 4 kcal/mol of translational energy is required to scatter C_3H_2N photoproducts to this angle, making our determination

of the $P(E_T)$ insensitive to total kinetic energies below 4 kcal/mol. The $P(E_T)$ for the H atom elimination channel as shown in Fig. 3 is monotonically decreasing out to a maximum of about 40 kcal/mol. The photoionization spectrum for the C_3H_2N photoproducts collected at a scattering angle of 7.5° is shown as the circles in Fig. 4. Taking into consideration the width of the undulator radiation, the photoionization onset is 9.3±0.3 eV.

The observed photoionization onsets depends on a combination of energetic factors in addition to the intrinsic photoionization potential of the detected species. We use the following expression to calculate the available energy,

$$E_{available} = E_{h\nu} - D_o(H\text{-}C_3H_2N) + E_{parent} \qquad \text{(eqn. 1)}$$

Estimating $D_o(H\text{-}C_3H_2N)$ to be 108 kcal/mol based on the C-H bond strength in ethylene[17] and neglecting the internal excitation of the parent molecule in the supersonic expansion[20], the available energy following H-atom elimination at 193 nm is about 40 kcal/mol. A minimum of 13 kcal/mol of translational energy is required to scatter a C_3H_2N photoproduct to 7.5°. The portion of the measured $P(E_T)$ above 13 kcal/mol has an average of $\langle E_T \rangle_{(>13\ kcal/mol)}$ = 20 kcal/mol. Since this channel results from atomic elimination and there is no evidence for electronic excitation of the products, any portion of the available energy not partitioned into translation must be partitioned into internal degrees of freedom in the C_3H_2N products. Subtracting the average translational energy from the available energy leaves an average internal energy in the C_3H_2N photoproducts detected at 7.5° of 20 kcal/mol. Therefore, the photoionization spectrum for m/e 52 photoproducts in Fig. 4 represents C_3H_2N radicals containing a very broad internal energy distribution with $\langle E_{int} \rangle$~20 kcal/mol. Without quantitative information about the effect of internal energy in the neutral C_3H_2N products on the photoionization process we are unable to report a corrected value for the photoionization onset of internally cold C_3H_2N radicals. However, additional internal energy will most likely lead to a red shift in the photoionization onset, and therefore our measured value of 9.3±0.3 eV should be considered a lower limit to the IP of cold C_3H_2N radicals. Using electron impact, Monigny

et al.[21] reported an appearance potential of 13.82 ±0.08 eV for $C_3H_2N^+$ from acrylonitrile, $C_3H_3N \rightarrow C_3H_2N^+ + H$. Subtracting the [estimated] C-H bond energy, $D_o(H\text{-}C_3H_2N)$=4.69 eV, the result suggest an IP for C_3H_2N of 9.1 eV in good agreement with our measured photoionization onset.

Molecular hydrogen elimination. Figure 5 shows TOF spectra for m/e 51 (C_3HN^+) at a source angle of 7.5° for photoionization energies of 12.0 eV and 14.0 eV, and a source angle of 10° for a photoionization energy of 12.0 eV. There are two contributions in the forward convolution fit to the TOF spectra. The major component in the fit is the result of H_2 elimination and was fitted with the $P(E_T)$ in Fig. 6. The $P(E_T)$ has a maximum probability at 18 kcal/mol and extends beyond 47 kcal/mol with $\langle E_T \rangle$=23±1 kcal/mol. The cross-hatched region shows the range in the $P(E_T)$ which leads to a reasonable fit to the TOF data. The minor component in the fit is the result of dissociative photoionization of C_3H_2N products that resulted from atomic hydrogen elimination and was fitted with the $P(E_T)$ in Fig. 3. Compared with the spectra at 12.0 eV, the 14.0 eV spectrum was well fitted by increasing the contribution of the dissociative ionization channel from the atomic hydrogen elimination products with respect to the H_2 elimination channel. Fitting spectra taken at both 12.0 eV and 14.0 eV, where the ratio of the two contributions to the signal is significantly different, provided additional confidence in the fit to the H_2 elimination channel. The photoionization spectrum for C_3HN photoproducts collected at a scattering angle of 10° is shown as the triangles in Fig. 4. The spectrum shows a photoionization onset of 10.8±0.3 eV. This is consistent with the IP for cyanoacetylene of 11.6 eV[17] with the red shift in the photoionization onset resulting from internal excitation in the HCCCN photoproducts.

HCN and CN elimination. There are two possible product channels which can result in a photoproduct mass combination of m/e 27 + m/e 26: HCN + C_2H_2 or C_2H_3 + CN. In traditional PTS experiments that employ electron impact product ionization it is often difficult or impossible to distinguish between dissociation channels that generate the same mass combination. The selectivity afforded by tunable VUV photoionization

provides a significant advantage in such cases. The photoionization spectrum for m/e 27 photoproducts collected at a scattering angle of 15° is shown in Fig. 7. The spectrum has a dominant feature with an onset around 11.0 eV and a small shoulder with an onset around 8.5 eV. The two possible photoproducts at m/e 27 are HCN and the vinyl radical, which have ionization potentials of 13.6 eV and 8.6 eV, respectively.[17] The shoulder with a photoionization onset around 8.5 eV is consistent with the IP for vinyl radicals. It cannot result from HCN photoproducts since a red shift of 5.1 eV from the HCN IP of 13.6 eV exceeds the available energy following photodissociation at 193 nm. The dominant feature in Fig. 7, with a photoionization onset around 11.0 eV, can be assigned to HCN photoproducts with the red shift of the photoionization onset reflecting substantial internal excitation in the HCN products. Additional evidence for the presence of two distinct dissociation channels leading to m/e 27 photoproducts is shown in Fig. 8. Figure 8 shows TOF spectra for m/e 27 at a source angle of 20° and at photoionization energies of 10.0 eV and 15.0 eV. The two spectra have been separately normalized in Fig. 8, although after kinematic and ionization intensity corrections, the signal observed at 10.0 eV photoionization energy was more than 100 times weaker than the signal at 15 eV. It is clear in Fig. 8 that at photoionization energies well above the IP for both HCN and the vinyl radical the m/e 27 TOF spectrum is dominated by HCN photoproducts. However, when the photoionization energy is set below the IP of HCN and above the IP for vinyl radicals, a very different TOF spectrum is observed, which we attribute to the vinyl + CN dissociation channel. It should be noted that selective ionization is essential to distinguish these channels, since the minor radical channel is lost in the tail of the dominant molecular channel without selective ionization.

HCN elimination. Figure 9 shows TOF spectra for m/e 27 photoproducts at source angles of 30° and 50° and a photoionization energy of 15 eV. As discussed above, at a photoionization energy of 15.0 eV the spectra in Fig. 9 are completely dominated by HCN photoproducts. Figure 10 shows TOF spectra for m/e 26 at source angles of 30° and 50° and a photoionization energy of 15 eV. The TOF spectra in Fig. 9 and 10 were fitted with the $P(E_T)$ in Fig. 11, confirming the TOF spectra in Fig. 10 to be the momentum

matched C_2H_2 partner fragment to HCN photoproducts. While 15.0 eV is sufficient to photoionize both C_2H_2 and CN photoproducts (the ionization potentials are 11.4 eV and 14.1 eV, respectively[17]) no difference in the shape of the m/e 26 TOF spectra was found when decreasing the photoionization energy to 12.0 eV. Since 12.0 eV is well below the IP for CN products, this confirms that the m/e 26 TOF spectra consist almost exclusively of C_2H_2 photoproducts from HCN elimination. The $P(E_T)$ for HCN elimination in Fig. 11 has a maximum probability at 8 kcal/mol, $\langle E_T \rangle$ = 15 kcal/mol, and decreases out beyond 47 kcal/mol. The cross-hatched region shows the range in the $P(E_T)$ about which a reasonable fit to the TOF data can be achieved. The photoionization spectrum for the m/e 26 (C_2H_2) photoproducts scattered to a laboratory angle of 15° is shown as the circles in Fig. 12. For comparison, the photoionization spectrum obtained by sending a neat molecular beam of acetylene directly into the detection region of the instrument and is shown as the triangles in Fig. 12. The two ionization spectra in Fig. 12 have been arbitrarily scaled to the integrated signal at a photoionization energy of 13.0 eV. The photoionization spectrum for acetylene has an abrupt onset at the IP for acetylene of 11.4 eV.[17] A more gradual onset is exhibited by the C_2H_2 photoproducts, starting at 10.5±0.3 eV. Based on this red-shift in the ionization potential we estimate that an appreciable fraction of the C_2H_2 products contain at least 1 eV of internal energy.

CN elimination. As discussed above, by tuning the photoionization energy below the onset for HCN photoproducts it is possible to discriminate against HCN photoproducts at m/e 27 enabling the measurement of TOF spectra for vinyl radical photoproducts that result from CN elimination. Figure 13 shows TOF spectra for m/e 27 ($C_2H_3^+$) photoproducts at source angles of 10° and 20° and a photoionization energy of 10.0 eV. The TOF spectra in Fig. 13 were fitted with the $P(E_T)$ shown as the solid line in Fig. 14. The $P(E_T)$ has a maximum probability at 1 kcal/mol and decreases out to a maximum translational energy of ~12 kcal/mol. Since CN has an IP of 14.1 eV[17] which lies above the IP of all of the possible C_2H_2 photoproducts, we were not able to discriminate against the C_2H_2 photoproducts from HCN elimination at m/e 26 in order to obtain TOF spectra for CN photoproducts.

The endothermicity, available energy, and average translational energy release for each of the observed dissociation channels are shown in table 1.

4. Discussion

A. Radical Elimination Channels

Hydrogen atom elimination. The $P(E_T)$ for hydrogen atom elimination shown by the solid line in Fig. 3 has a maximum probability ≤4 kcal/mol and decreases out to ~40 kcal/mol. Translational energy distributions of this type are indicative of simple bond rupture on the ground electronic surface involving little or no barrier to recombination and near statistical partitioning of the available energy. For comparison, the statistical prediction from a prior distribution[22] is shown as the dashed line in Fig. 3. Since we do not measure the complete $P(E_T)$ (we cannot measure below 4 kcal/mol) we were not able to normalize the measured $P(E_T)$ with respect to the statistical prediction. We have arbitrarily scaled the two distributions in Fig. 3 to match at 6 kcal/mol.

A prior distribution for the available energy of 40 kcal/mol predicts $\langle E_T \rangle = 4$ kcal/mol. The measured $P(E_T)$ does not fall off above 4 kcal/mol as rapidly as the prior model which indicates that slightly more energy is partitioned into the translational degrees of freedom than the statistical expectation. One possible explanation for the excess kinetic energy would be a small recombination barrier. Alternatively, the classical treatment of high frequency oscillators in the prior model may overestimate the vibrational energy in C_3H_2N, leading to an underestimate of the translational energy.

While there have been no previous reports of measurements of this dissociation channel, our measured $P(E_T)$ is very similar to the $P(E_T)$ measured by Balko *et al.*[1] for hydrogen atom elimination from ethylene at 193 nm. Interestingly, Mo *et al.* reported a translational energy distribution based on hydrogen atom Doppler profiles from the dissociation of vinyl chloride at 193 nm which were consistent with a Maxwell-Boltzmann distribution and contained an average translational energy of 17 kcal/mol.[23] This very large

fraction of the available energy, 35% on average, in translation would seem to indicate a nonstatistical partitioning of the available energy suggesting a significant difference in the mechanism of hydrogen atom elimination from vinyl chloride as compared with acrylonitrile and ethylene. The hydrogen atom Doppler profiles were isotropic which was considered an indication of internal conversion prior to dissociation. This result is consistent with our measured $P(E_T)$ for acrylonitrile and the measured $P(E_T)$ for ethylene, that suggest internal conversion to the ground electronic surface prior to C-H bond cleavage. Using the same technique as in this study, we have investigated the dissociation of vinyl chloride at 193 nm.[24] Although we were not able to measure the complete $P(E_T)$ for the H atom elimination channel, the portion of the $P(E_T)$ which we were able to measure is consistent with statistical bond rupture on the ground electronic surface and contradicts the large average translational energy release reported in the Doppler study. Our results indicate that the primary hydrogen atom elimination channel in both acrylonitrile and vinyl chloride (as well as in ethylene) involve very similar mechanisms.

CN elimination. The minor CN elimination channel in acrylonitrile has been reinvestigated recently.[9,10] North and Hall[10] measured a CN quantum yield of 0.003 ±0.001 in stark contrast to the earlier PTS study of Nishi *et al.* who had assigned a CN quantum yield of 0.75 based on indirect TOF evidence.[7] Although we lack quantitative information concerning the photoionization cross sections of the products, we estimate this channel to account for <1% of the total dissociation yield at 193 nm in agreement with the results of North and Hall. The CN elimination channel is substantially smaller than the analogous Cl elimination channel in vinyl chloride, which may account for as much as 50% of the dissociation products at 193 nm.[25] In vinyl chloride the large Cl elimination channel is due to the participation of a direct dissociative state which crosses the initially excited $\pi\pi^*$ state in the Franck-Condon region.[3,4,25] The absence of such a repulsive electronic surface correlating to CN elimination in acrylonitrile forces this channel to compete with other more energetically favorable dissociation pathways on the ground state potential energy surface. As a result, the molecular elimination channels dominate and the radical channels are relatively minor.

The translational energy distribution determined in this experiment is consistent with the statistical randomization of the available energy followed by a barrierless dissociation on the ground electronic state. A prior translational energy distribution[22], which approximates a statistical partitioning of energy, is shown as the dash-dot line in Fig. 14 and is qualitatively very similar to the measured distribution (solid line). For comparison, an impulsive model[26] which has been invoked to fit the fast Cl elimination channel in vinyl chloride, would result in an average translational energy of ~9 kcal/mole, rather than the 2.4 kcal/mole observed. Furthermore, in such cases the $P(E_T)$ most often resembles a Gaussian distribution centered at the impulsive average, qualitatively dissimilar to the experimental observations.

State-dependent translational distribution from the analysis of Doppler profiles over the range of populated CN rotational states in v=0 have been recently measured by North and Hall.[10] The state-dependent distributions were indistinguishable, suggesting that the $P(E_T)$ derived from a single CN state can be compared to the present, state-averaged, measurements. The $P(E_T)$ obtained from CN Doppler profiles for N=24, v=0 is shown as the dashed line in Fig. 14. The present experimental distribution is slightly colder than the Doppler measurement. The small difference may simply be due to the contribution of $v \geq 1$ and the supersonic cooling of the parent molecule in the PTS measurements.

B. Molecular Elimination Channels

HCN elimination. Thermodynamically there are three C_2H_2 isomers that can be produced from the elimination of HCN following absorption at 193 nm, reactions 5-7:

$H_2CCHCN \rightarrow HCCH + HCN$ $\quad \Delta H_0 = 43.0$ kcal/mol (rxn 5)

$H_2CCHCN \rightarrow :CCH_2\ (^1A_1) + HCN$ $\quad \Delta H_0 = 86$ kcal/mol (rxn 6)

$H_2CCHCN \rightarrow :CCH_2\ (^3B_2) + HCN$ $\quad \Delta H_0 = 134$ kcal/mol (rxn 7)

The $P(E_T)$ for HCN elimination in Fig. 11 has a maximum probability at 8 kcal/mol, extends beyond 47 kcal/mol, and has a FWHM of ~20 kcal/mol. The available energy for reaction 7 is only 14 kcal/mol. Since 50% of the $P(E_T)$ lies above 14 kcal/mol we can place an upper limit on the contribution of reaction 7 at half of the total HCN elimination based on energy conservation. The photoionization spectra for the C_2H_2 photoproducts, shown in Fig. 12, has an onset at 10.5±0.3 eV. Although the ionization potential for singlet and triplet vinylidene are not well determined, we have adopted a value of 11.4 eV for the IP of singlet vinylidene based on the recommended value from Romus *et al.*[27] If we assume that the IP for triplet vinylidene is the IP for singlet vinylidene reduced by the singlet/triplet splitting energy of 2.0 eV[29] we obtain an estimate of 9.4 eV for the IP of triplet vinylidene. Our measured photoionization onset is 1 eV above this estimate for the IP of triplet vinylidene. Considering the thermodynamic restrictions and the failure to observe any signal within 1 eV above our estimated value for the IP of triplet vinylidene, we believe that reaction 7 is not a significant channel in HCN elimination. This is contrary to the conclusion of Fahr and Laufer, who reported that this was the major HCN elimination pathway following VUV flash photolysis.[2] While we can rule out the participation of reaction 7 in acrylonitrile dissociation, energy conservation alone cannot distinguish between reactions 5 (1,1 elimination) and 6 (1,2 elimination).

Several pieces of evidence lead us to favor a 1,1 elimination mechanism for the production of HCN and C_2H_2. Recent *ab initio* calculations have found the transition state for reaction 6 at 107 kcal/mol and the transition state for reaction 5 at 116 kcal/mol.[28] RRKM rate calculations, using the *ab initio* transition state frequencies and energetics, led to a rate about 100 times slower for reaction 5 than for reaction 6. Although not conclusive, the calculated rates strongly suggest that reaction 6 is the dominant HCN elimination channel. The calculated values for the transition states of reactions 6 and 5 provide recombination barrier heights of 19 and 71 kcal/mol, respectively. Since a large fraction of the recombination barrier typically appears as product translation, the observed average translational energy release of 15 kcal/mol is

consistent with 1,1 HCN elimination, and much smaller than what one might expect from 1,2 elimination. The evidence in favor of a 1,1 HCN elimination mechanism is clouded, however, by the internal energy estimates derived from the photoionization threshold spectra. If dissociation produced HCN and singlet vinylidene with15 kcal/mole average translational energy, the nascent products should divide the remaining 46 kcal/mole between the internal degrees of freedom of the two fragments. Isomerization of singlet vinylidene to acetylene[29] would be complete prior to photoionization detection, and an additional 43 kcal/mole of isomerization energy should be depositied in the C_2H_2 vibrational energy. The ionization onsets observed suggest that the HCN is too hot and the C_2H_2 is too cold for this mechanism.

The interpretation of large red-shifts in the photoionization onsets is somewhat problematic, and deserves some discussion. The photoionization onset for HCN products, the major feature in figure 7, exhibits a reduction of 2.6 eV (60 kcal/mol) from the IP of HCN = 13.6 eV (ref 17). Our measured photoionization onset of 10.5±0.3 eV for the C_2H_2 species is 0.9 eV (21 kcal/mol) below the IP for acetylene. We note that the sum of the average translational energy and the two photoionization onset red-shifts is very close to the 104 kcal/mol available energy, encouraging the use of the reduction in the photoionization onset as a qualitative estimate of product internal energy. Quantitative interpretation of such red shifts would depend on a detailed analysis of the autoionization of vibrationally excited Rydberg levels which could generally be accessed with approximately diagonal Franck-Condon transitions, as well as a Franck-Condon analysis of direct photoionization. We do not attempt this difficult analysis, but note that the influence of photofragment internal energy on photoionization threshold spectra is an issue that will affect many PTS and crossed beam scattering experiments that use tunable VUV product photoionization, and deserves further study. For our present purposes, we merely note that a 2.6 eV red shift in the HCN ionization onset implies an internal energy far too large to be consistent with the direct formation of HCN and singlet vinylidene.

A resolution of this apparent contradiction comes from a recognition of the low barrier and rapid isomerization rate of singlet vinylidene to acetylene. Based on negative

ion photodetachment spectral linewidths, Lineberger and coworkers estimated a lifetime of 40-200 fs for the isomerization of vinylidene to acetylene.[29] Given the extremely short lifetime of singlet vinylidene, it may not be appropriate to think of the dissociation and the isomerization of the C_2H_2 product as temporally separated processes. As a result, some fraction of the isomerization energy would be available for partitioning into degrees of freedom other than internal excitation of the acetylene product, in agreement with our estimate of the acetylene and HCN internal energies. A concerted mechanism of this type is analogous to the HCl elimination mechanism from vinyl chloride proposed by Gordon and coworkers.[4]

Comparison of our measured $P(E_T)$ for the HCN + C_2H_2 channel with the previous PTS experiments of Nishi *et al.*[7] show disagreement at two levels. To begin with, the m/e 27 measurements were attributed to a superposition of HCN from reaction 4 with C_2H_3 from reaction 2. From the CN quantum yield measurements of North and Hall[10] and the selective ionization studies reported here, it is now clear that the m/e 27 TOF signals reported by Nishi *et al.* were dominated by HCN. Second, if reinterpreted as a single distribution for the HCN elimination channel, the total $P(E_T)$ should then be comparable to our HCN measurements shown in Fig. 11. The total $P(E_T)$ reported by Nishi *et al.* is substantially colder than our measurements, with a maximum near 3 kcal/mole, compared to 8 kcal/mol in our measurements. One possible explanation for the slower $P(E_T)$ presented by Nishi *et al.* could come from the long-time tails on their TOF spectra which were attributed to residual gas buildup following the molecular beam pulse. A direct inversion of these TOF spectra to obtain translational energy distributions may have been biased toward lower energy.

Gordon and coworkers measured the state selected $P(E_T)$ for HCl(v=0, v=1, and v=2) from vinyl chloride dissociation at 193 nm using Doppler spectroscopy.[3] The shape of the distributions are very similar to our measured $P(E_T)$ from HCN elimination with a slightly higher average translational energy which is consistent with the higher available energy for the elimination of HCl from vinyl chloride of 124 kcal/mol compared to 104 kcal/mol for acrylonitrile. The agreement between the analogous HCN and HCl

translational energy distributions suggests the two dissociations proceed *via* a very similar mechanism on the ground electronic surface.

Molecular hydrogen elimination. The elimination of H_2 from acrylonitrile at 193 nm can give rise to three C_3HN isomers,

$H_2CCHCN \rightarrow HCCCN + H_2$	$\Delta H_0 = 50$ kcal/mol	(rxn 8)
$H_2CCHCN \rightarrow {}^1(:CCHCN) + H_2$	ΔH_0 ~90 kcal/mol	(rxn 9)
$H_2CCHCN \rightarrow {}^3(:CCHCN) + H_2$	ΔH_0 ~140 kcal/mol	(rxn 10)

We can estimate the endothermicity for dissociation to give of H_2 and singlet cyanovinyl radical, reaction 9, based on the endothermicity of the analogous H_2 elimination from ethylene and vinyl chloride.[1,30] We assume that the singlet/triplet splitting in the cyanovinyl radical is similar to the singlet/triplet splitting in vinylidene of 48 kcal/mol[29] to obtain the estimated endothermicity of reaction 10. The $P(E_T)$ for molecular hydrogen elimination is shown in Fig. 6. The available energy following reaction 10 is ~8 kcal/mol. Since all the photofragments from this channel have translational energy in excess of the energetic limit of reaction 10 it is unlikely that this reaction plays a significant role in H_2 elimination. The $P(E_T)$ is consistent with the energetics of both remaining channels. The measured width and peak position of the $P(E_T)$ suggest the presence of a large recombination barrier.

Similar arguments can be made about the expected kinetic energy release for 1,1 vs. 1,2 elimination of H_2 that were made above for the 1,1 vs. 1,2 elimination of HCN. Strong repulsion between closed-shell H_2 and cyanoacetylene at small distances are responsible for a large recombination barrier in the 1,2 H_2 elimination, reaction 8. A recombination barrier to 1,1 H_2 elimination has been calculated by Riehl *et al.*[30] to be about 6 kcal/mol in the vinly chloride ground state. By analogy, we expect the recombination barrier to 1,1 H_2 elimination in acrylonitrile also to be much smaller than for 1,2 elimination. However, as in the case of vinylidne/acetylene isomerization, the

cyanovinyl radical can also isomerize rapidly to cyanoacetylene, allowing the two photofragments to experience part of the strong repulsive potential between H_2 and cyanoacetylene at close proximity. A barrier of only about 1 kcal/mol for the analogous chlorovinyl to chloroacetylene isomerization has also been calculated by Riehl *et al.* The magnitude of the repulsion between H_2 and cyanoacetylene will be strongly dependent on the rate of isomerization with respect to the rate of product separation. The result of such a concerted elimination/isomerization process should be the partitioning of some of the energy of isomerization into translation of the dissociating fragments. In the study of ethylene dissociation at 193 nm, isotopically labeled reagents demonstrated a 3:2 preferences for 1,1 vs. 1,2 H_2 elimination, while the measured $P(E_T)$ was a single broad feature peaked around 20 kcal/mol.[1] These results show that despite the large difference in the two recombination barriers, the coupling of isomerization to 1,1 elimination can result in comparable kinetic energies for the two competing mechanisms. A similar situation seems likely in the case of acrylonitrile.

An alternative reaction pathway consistent with a large recombination barrier is H-atom migration to form the cyanoethylidene radical followed by H_2 elimination. From thermodynamic arguments and H_2 rotational populations, Gordon and coworkers also found evidence for both 3 and 4 center H_2 elimination mechanisms in the dissociation of vinyl chloride.[3] The authors suggested the most likely path for 3 center elimination involved an initial H-atom migration followed by dissociation. The barrier to H-atom migration in vinyl chloride was calculated by Reihl *et al.* to lie below all of the barriers to dissociation.[30] We are unable to distinguish between a 3 center elimination that follows H-atom migration and a rapid isomerization of singlet vinylidene in concert with 1,1 H_2 elimination based on our measured $P(E_T)$. In the limit of a short lifetime for the chloroethylidene radical intermediate the two mechanisms become essentially identical.

The photoionization spectrum for C_3HN photoproducts, triangles in Fig. 4, has a photoionization onset of 10.8±0.3 eV. Any cyanovinyl radicals formed will isomerize prior to reaching the photoionization region. Therefore, in the case of either 1,1 or 1,2 H_2 elimination cyanoacetylene will be detected as the final product. The photoionization onset

for cyanoacetylene is red shifted from its IP of 11.6 eV[17]. If the red shift of 0.8 eV can be associated with the internal energy this would suggest that in the case of 1,1 H_2 elimination, reaction 9, only about half of the isomerization energy from the cyanovinyl radical to cyanoacetylene, ΔH_I ~2 eV[29], is partitioned into internal energy of the cyanoacetylene products on average. Although the 1,2 elimination would be expected to have a larger translational energy release then 1,1 elimination, with $\langle E_T \rangle$=23 kcal/mol in Fig. 6 there is still ~75 kcal/mol of available energy on average to be partitioned into internal energy of the H_2 and cyanoacetylene. Using 0.8 eV (18 kcal/mol) as a qualitative estimate of the internal energy content in cyanoacetylene leaves over half of the available energy partitioned into internal excitation of the H_2 products on average, ~56 kcal/mol.

C. Overview of the Dissociation Mechanism

We now attempt to summarize the mechanism for acrylonitrile dissociation following excitation at 193 nm. Although we have not performed measurements of the photofragment anisotropy in this study, there is significant evidence that the dissociation produces an isotropic distribution of fragments. Measurement of the photofragment anisotropies for H and H_2 elimination channels are notoriously difficult due to the low center of mass recoil of the heavy fragments which we detect. However, the analogous channels in the photodissociation of vinyl chloride are isotropic. North and Hall failed to detect any anisotropy in careful polarization measurements of CN Doppler profiles. This observation was consistent with the derived speed distribution, confirmed in the present work, which indicated a statistical partitioning of the available energy and suggested that CN elimination occurred on the ground electronic state. The photofragment angular distribution for the HCN elimination channel was found by Nishi *et al.* to also be isotropic. The lack of anisotropy in all dissociation channels in acrylonitrile suggests that the excited molecule is long lived on the time scale of molecular rotation which is consistent with an electronic predissociation mechanism, involving either internal conversion or intersystem crossing prior to dissociation. If internal conversion occurs, acrylonitrile photodissociation

at 193 nm represents a means to examine the competition between ground state reaction pathways starting from a well defined microcanonical ensemble. In order for this model to be correct the product branching ratios must be consistent with the corresponding microcanonical rates. RRKM calculations using transition state energies and frequencies for the CN elimination and 1,1 HCN elimination channels give rates in a ratio of $2x10^{-4}$:1.[28] This is in agreement with the reported CN:HCN product branching ratio. Without photoionization cross section information, we are unable to assign experimental estimates for the relative amounts of H and H_2 loss channels compared to the CN and HCN channels. Work is in progress to characterize all relevant transition states for the dissociation of acrylonitrile.

5. Conclusion

Using the technique of photofragment translational spectroscopy with VUV photoionization of the products we have identified four dissociation channels following absorption at 193 nm, reactions 1-4. All four dissociation channels are consistent with internal conversion to the ground electronic surface following the initially optically prepared state. The molecular dissociation channels have $P(E_T)$'s that reflect large recombination barriers. Based on calculated barrier heights, the HCN elimination channel should be dominated by 1,1 HCN elimination. In the case of 1,1 HCN elimination, the dissociation proceeds to give singlet vinylidene in a dissociation that involves concerted isomerization to acetylene analogous to the mechanism proposed by Gordon and coworkers for HCl elimination from vinyl chloride. The isomerization proceeds on the time scale of photofragment separation allowing some portion of the isomerization energy to be partitioned into degrees of freedom other than internal energy of the acetylene product. A very large fraction of the available energy, >50%, is partitioned into internal energy of the HCN photoproduct. Although we do not have conclusive evidence for the reaction mechanism associated with H_2 elimination, the H_2 elimination channel is consistent with competing 3 and 4 center elimination processes. Akin to the 1,1 HCN

elimination, a 1,1 H_2 elimination channel must result in formation of the singlet cyanovinylidene radical with rapid isomerization to cyanoacetylene. The concerted isomerization/dissociation would again allow the energy of isomerization to be partitioned into all of the available degrees of freedom. We found over 50% of the available energy partitioned into internal degrees of freedom in the H_2 product. Atomic hydrogen elimination exhibits a $P(E_T)$ which is consistent with statistical simple bond rupture. The distribution maximum is shifted to slightly higher energy than the prior model prediction, which may indicate the presence of a small recombination barrier. The radical CN elimination channel accounts for a very small fraction of the dissociation, <1%. The measured translational energy release is similar to the statistical prediction of a prior distribution, indicating a barrierless dissociation on the ground electronic surface.

Acknowledgments

This work was supported by the Director, Office of Energy Research, Office of Basic Energy Science, Chemical Sciences Division of the U. S. Department of Energy under contract No. DE-AC03-76SF00098. The experiments were conducted at the Advanced Light Source, Lawrence Berkeley National Laboratory which is supported by the same source. Work by SWN and GEH at Brookhaven National Laboratory was performed under contract No. DE-AC02-76CH00016 with the U.S. Department of Energy and supported by its Chemical Sciences Division. The authors wish to thank Dr. Michael Hall and the Laboratory for Molecular Simulation at Texas A&M University.

Table 1. Summary of translational energy release from the four observed dissociation channels. All values are in kcal/mol. Thermodynamic values were taken from reference 31 and available energies were calculated using equation 1.

Reaction Channel	ΔH_0	E_{avail} at 193 nm	$\langle E_T \rangle$	$\langle E_T \rangle / E_{avail}$
$H_2CCHCN \rightarrow H + H_2CCCN$	~108	~40	na	na
$H_2CCHCN \rightarrow CN + H_2CCH$	131	17	2.4	14
$H_2CCHCN \rightarrow H_2 + HCCCN$	50	97	23	24
$H_2CCHCN \rightarrow HCN + HCCH$	43.0	104.4	15	14

References

[1] B. A. Balko, J. Zhang, and Y. T. Lee, *J. Chem. Phys.* **97**, 935 (1992) *and references therein;* E. F. Cromwell, A. Stolow, M. J. J. Vrakking, and Y. T. Lee, *J. Chem. Phys.* **97**, 4029 (1992).

[2] A. Fahr and A. H. Laufer, *J. Photochem.* **34**, 261 (1989).

[3] M. J. Berry, *J. Chem. Phys.* **61**, 3114 (1974); Y. Huang, Y. Yang, G. He, S. Hashimoto, and R. J. Gordon, *J. Chem. Phys.* **103**, 5476 (1995) *and references therin*: G. He, Y. Yang, Y. Huang, S. Hashimoto, and R. J. Gordon, *J. Chem. Phys.* **103**, 5488 (1995).

[4] M. Umemoto, K. Seki, H. Shinohara, U. Nagashima, M. Kinoshita, and R. Shimada, *J. Chem. Phys.* **83**, 1657 (1985).

[5] P. A. Mullen and M. K. Orloff, Theoret. *Chim. Acta* **23**, 278 (1971).

[6] A. Gandini and P. A. Hackett, *Can. J. Chem.* **56**, 2069 (1978).

[7] N. Nishi, H. Shinohara, and I. Hanazaki, *J. Chem. Phys.* **77**, 246 (1982).

[8] A. Fahr and A. H. Laufer, *J. Phys. Chem.* **96**, 4217 (1992).

[9] C. A. Bird and D. J. Donaldson, *Chem. Phys. Lett.* **249**, 40 (1996).

[10] S. W. North and G. E. Hall, *Chem. Phys. Lett.* **263**, 148 (1996).

[11] D. A. Blank, S. W. North, D. Stranges, A. G. Suits, and Y. T. Lee, *J. Chem. Phys.* **106**, 539 (1997).

[12] X. Yang, D. A. Blank, J. Lin, P. A. Heimann, A. M. Wodtke, A. Suits, and Y. T. Lee, Rev. Sci. Instrum., *to be published.*

[13] A. M. Wodtke and Y. T. Lee, J. Phys. Chem. 89, 4744 (1985).

[14] Y. T. Lee, J. D. McDonald, P. R. LeBreton, and D. R. Herschback, Rev. Sci. Instrum. 40, 1402 (1969); N. R. Daly, *ibid* 31, 264 (1960).

[15] M. Koike, P. A. Heimann, A. H. Kung, T. Namioka, R. DiGennaro, B. Gee, N. Yu, Nuclear Instruments and Methods in Physics Research 347, 282 (1994).
P. A. Heimann, M. Koike, C. W. Hsu, M. Evans, C. Y. Ng, D. Blank, X. M. Yang, C. Flaim, A. G. Suits, Y. T. Lee, SPIE Proceedings 2865 (1996).

[16] A. G. Suits, P. Heimann, X. Yang, M. Evans, C. Hsu, K. Lu, and Y. T. Lee, Rev. Sci. Instrum. 66, 4841 (1995).

[17] Handbook of Chemistry and Physics, D. R. Lide (CRC, Boca Raton, 1995).

[18] J. A. R. Samson, *Techniques of Vacuum Ultraviolet Spectroscopy*, Wiley, New York, 1967.

[19] X. Zhao, Ph.D. Thesis, University of California, Berkeley (1989).

[20] At 273 K acrylonitrile will contain an average of 0.9 kcal/mol in rotation and 0.8 kcal/mol in vibration and the acrylonitrile reactant will experience substantial cooling upon supersonic expansion.

[21] J. Monigny, J. Urbain, and H. Wankenne, *Bull. Soc. Roy. Sci. Liege* **34**, 337 (1965).

[22] R. D. Levine and R. B. Bernstein, *Acc. Chem. Res.* **7**, 393 (1974); J. T. Muckerman, *J. Phys. Chem.* **93**, 179 (1989).

[23] Y. Mo, K. Tonokura, Y. Matsumi, M. Kawasaki, T. Sato, T. Arikawa, P. T. A. Reilly, Y. Xie, Y. Yang, Y. Huang, and R. J. Gordon, *J. Chem. Phys.* **97**, 4815 (1992).

[24] D. A. Blank, S. Weizhong, A. G. Suits, Y. T. Lee, S. W. North, and G. E. Hall, *manuscript in preparation.*

[25] M. Umemoto, K. Seki, H. Shinohara, U. Nagashima, N. Nishi, M. Kinoshita, and R. Shimada, *J. Chem. Phys.* **83**, 1657 (1985).

[26] G. E. Busch and K.R. Wilson, *J. Chem. Phys.* **56**, 3626 (1972).

[27] P. Romus, P. Botschwina, and J. P. Maier, *Chem. Phys. Lett.* **84**, 71 (1981).

[28] A. Deresckei-Kovacs and S. W. North, *manuscript in preparation.* The calculations were performed at the MP4/6-311++G** level of theory.

[29] K. M. Ervin, J. Ho, and W. C. Lineberger, *J. Chem. Phys.* **91**, 5974 (1989).

[30] J. Riehl and K. Morokuma, *J. Chem. Phys.* **100**, 8976 (1994).

[31] The heats of formation for acrylonitrile, acetylene, vinyl radical, HCN, H, and CN were taken from reference 17. The heat of formation for cyanoacetylene was obtain by group additivity from S. W. Benson, *Thermochemical Kinetics*, John Wiley & Son, Inc., 1968. The isomerization energy for acetylene/vinylidene and the singlet/triplet splitting for vinylidene were taken from reference 29.The dissociation energy for H_2 elimination to give both singlet and triplet cyanovinylidene were roughly estimated based on the dissociation energy for H_2 elimination from ethylene to give both singlet and triple vinylidene.

Figure Captions

Figure 1: The relative energy of possible dissociation channels from acrylonitrile following absorption at 193 nm. The origin of the thermodynamic values are in reference 31.

Figure 2: TOF spectra for m/e 52 ($C_3H_2N^+$) photoproducts at source angles of 5° and 7.5° and a photoionization energy of 14.0 eV. The solid line is the forward convolution fit using the $P(E_T)$ shown as the solid line in Fig. 3.

Figure 3: The solid line is the $P(E_T)$ used to fit the TOF spectra in Fig. 2 for hydrogen atom elimination, $C_3H_3N \rightarrow H + C_3H_2N$. The dotted line is the calculated prior distribution given an available energy of 40 kcal/mol for comparison.

Figure 4: The circles are the photoionization spectrum for the m/e 52 ($C_3H_2N^+$) photoproducts from hydrogen atom elimination, $C_3H_3N \rightarrow H + C_3H_2N$, at a source angle of 7.5°. The triangles are the photoionization spectrum for the m/e 51 (C_3HN^+) photoproducts from molecular hydrogen elimination, $C_3H_3N \rightarrow H_2 + C_3HN$, at a source angle of 10°.

Figure 5: TOF spectra for m/e 51 (C_3HN^+) photoproducts at source angle of 7.5° and a photoionization energies of 14.0 eV and 12.0 eV and at a source angle of 10° with a photoionization energy of 12.0 eV. The dotted line representing the larger contribution to the fits is the forward convolution fit using the $P(E_T)$ shown in Fig. 6 for molecular hydrogen elimination, $C_3H_3N \rightarrow H_2 + C_3HN$. The dotted line representing the smaller contribution to the fit is the result of dissociative ionization of C_3H_2N photoproducts resulting from

hydrogen atom elimination, $C_3H_3N \rightarrow H + C_3H_2N$, and was fitted with the $P(E_T)$ in Fig. 3. The solid line is the total forward convolution fit to the data.

Figure 6: The $P(E_T)$ for molecular hydrogen elimination, $C_3H_3N \rightarrow H_2 + C_3HN$, used for the forward convolution fits to the TOF spectra in Fig. 5.

Figure 7: The photoionization spectrum for m/e 27 photoproducts at a source angle of 15°. The major component with an onset ~11 eV is from HCN photoproducts, $C_3H_3N \rightarrow HCN + C_2H_2$, and the small shoulder with an onset at 8.5 eV is from vinyl radical photoproducts generated by CN elimination, $C_3H_3N \rightarrow CN + C_2H_3$.

Figure 8: TOF spectra for m/e 27 photoproducts at a source angle of 20° and photoionization energies of 10.0 eV, solid line, and 15.0 eV, dashed line. The TOF spectrum at 10.0 eV represents vinyl radical products from CN elimination and the spectrum at 15.0 eV is dominated by HCN photoproducts, see text. The two TOF spectra have been independently normalized, however the TOF spectrum at 10.0 eV has a corrected signal intensity <1% of the TOF spectrum at 15.0 eV.

Figure 9: TOF spectra for m/e 27 at source angles of 30° and 50° and a photoionization energy of 15.0 eV. The solid line is the forward convolution fit for HCN elimination, $C_3H_3N \rightarrow HCN(m/e\ 27) + C_2H_2(m/e\ 26)$, using the $P(E_T)$ in Fig. 11.

Figure 10: TOF spectra for m/e 26 at source angles of 30° and 50° and a photoionization energy of 15.0 eV. The solid line is the forward convolution fit for HCN

elimination, $C_3H_3N \rightarrow HCN(m/e\ 27) + C_2H_2(m/e\ 26)$, using the $P(E_T)$ in Fig. 11.

Figure 11: The $P(E_T)$ for HCN elimination, $C_3H_3N \rightarrow HCN + C_2H_2$, used for the forward convolution fits to the TOF spectra in Fig. 9 and 10.

Figure 12: The circles are the photoionization spectrum for m/e 26 photoproducts at a source angle of 15°. The triangles are the photoionization spectrum for a molecular beam of acetylene.

Figure 13: TOF spectra for m/e 27 at source angles of 10° and 20° and a photoionization energy of 10.0 eV. The solid line is the forward convolution fit for CN elimination, $C_3H_3N \rightarrow CN(m/e\ 26) + C_2H_3(m/e\ 27)$, using the $P(E_T)$ represented by the solid line in Fig. 14. Note that 10.0 eV is below the IP for HCN thereby discriminating against the HCN elimination channel at m/e 27.

Figure 14: The solid line is the $P(E_T)$ for CN elimination, $C_3H_3N \rightarrow CN + C_2H_3$, used for the forward convolution fits to the TOF spectra in Fig. 13. The dashed line is the $P(E_T)$ for CN elimination determined by Doppler spectroscopy by North and Hall. The dash-dot-dash line is the calculated prior distribution assuming 18 kcal/mol of available energy.

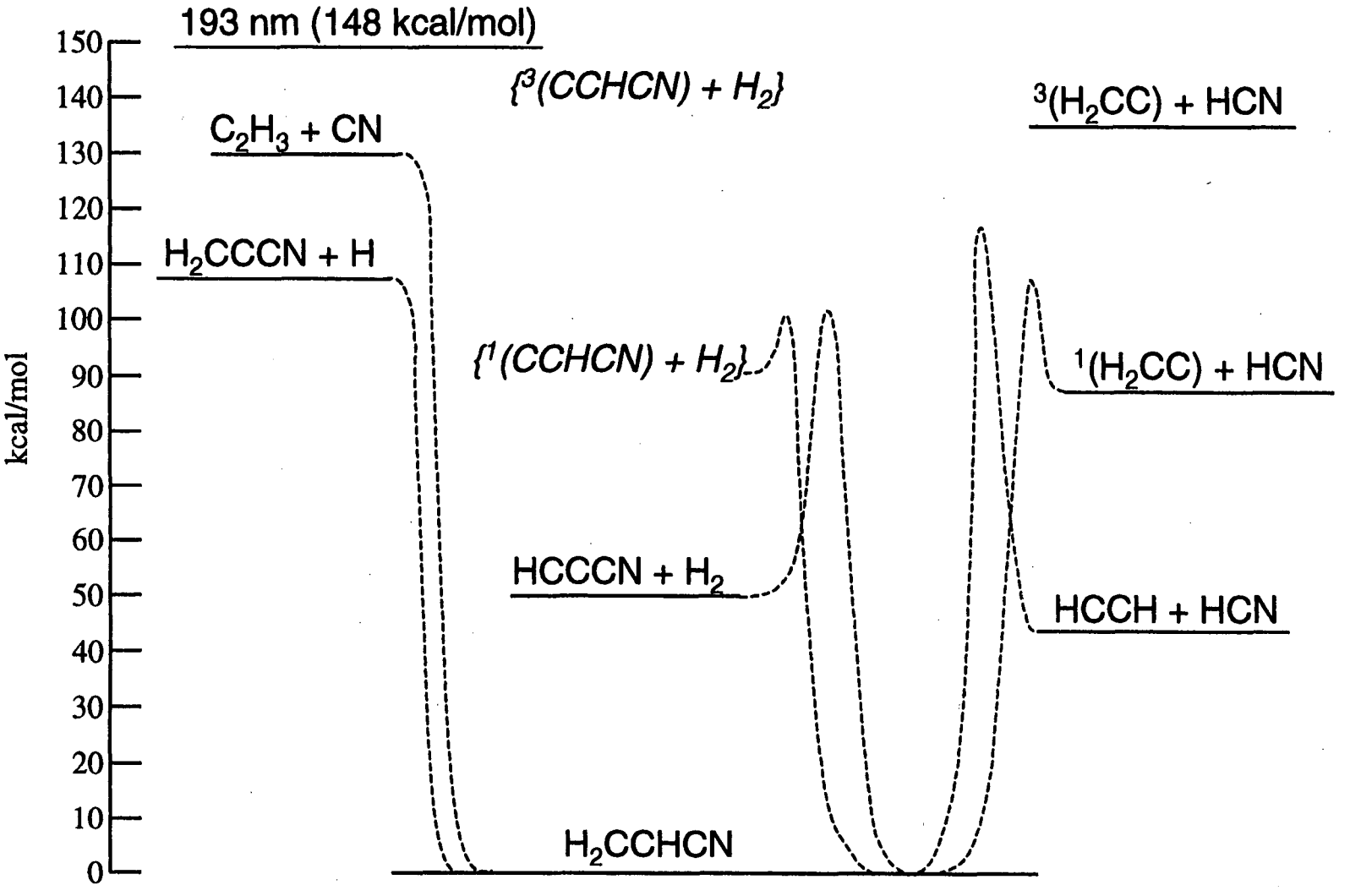
193 nm (148 kcal/mol)
kcal/mol
150
140
130
120
110
100
90
80
70
60
50
40
30
20
10
0
C2H3 + CN
H2CCCN + H
{3(CCHCN) + H2}
{1(CCHCN) + H2}
HCCCN + H2
H2CCHCN
3(H2CC) + HCN
1(H2CC) + HCN
HCCH + HCN

figure 1

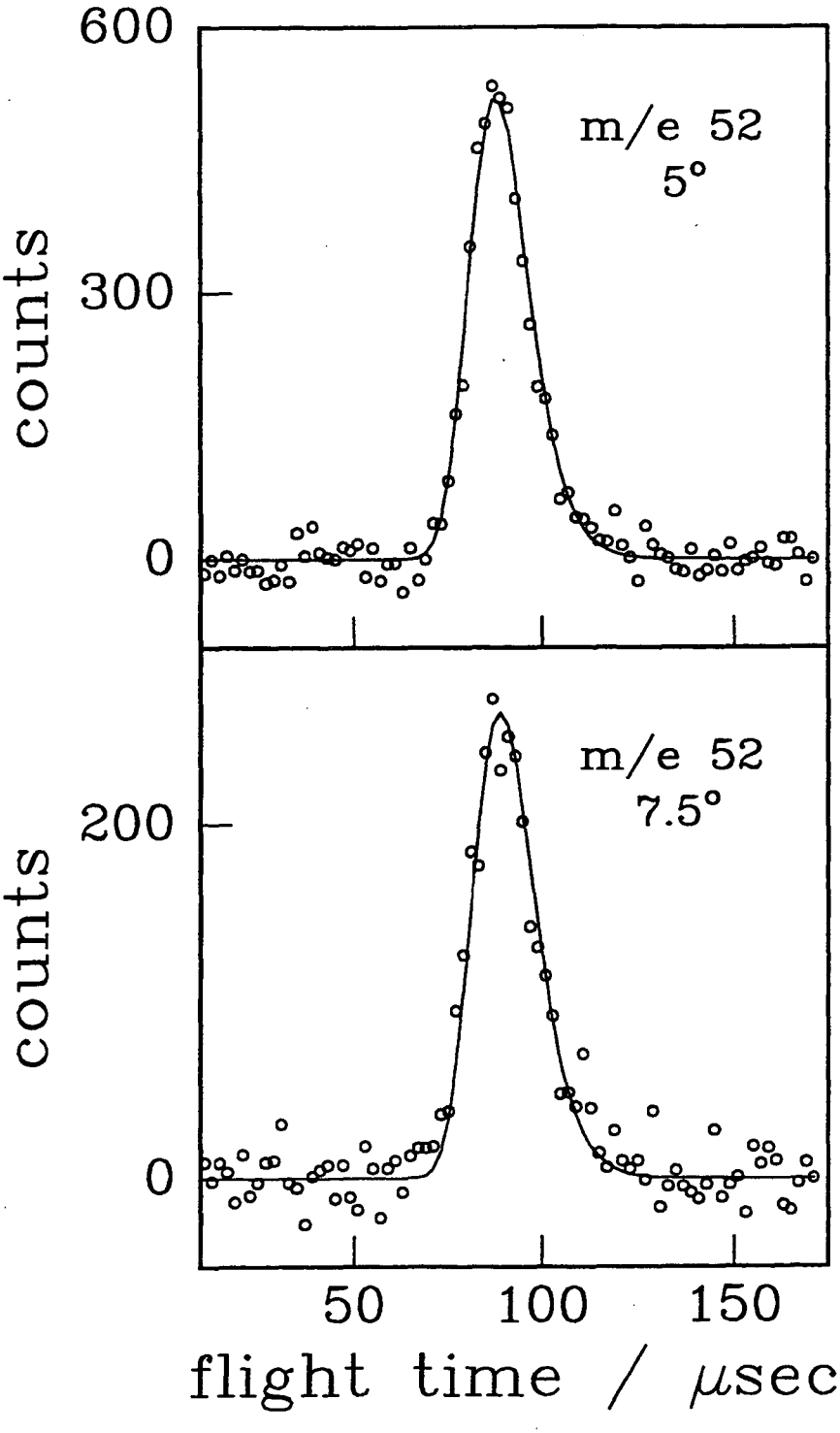
600
300
0
counts
m/e 52
5°
200
0
counts
m/e 52
7.5°
50
100
150
flight time / μsec

figure 2

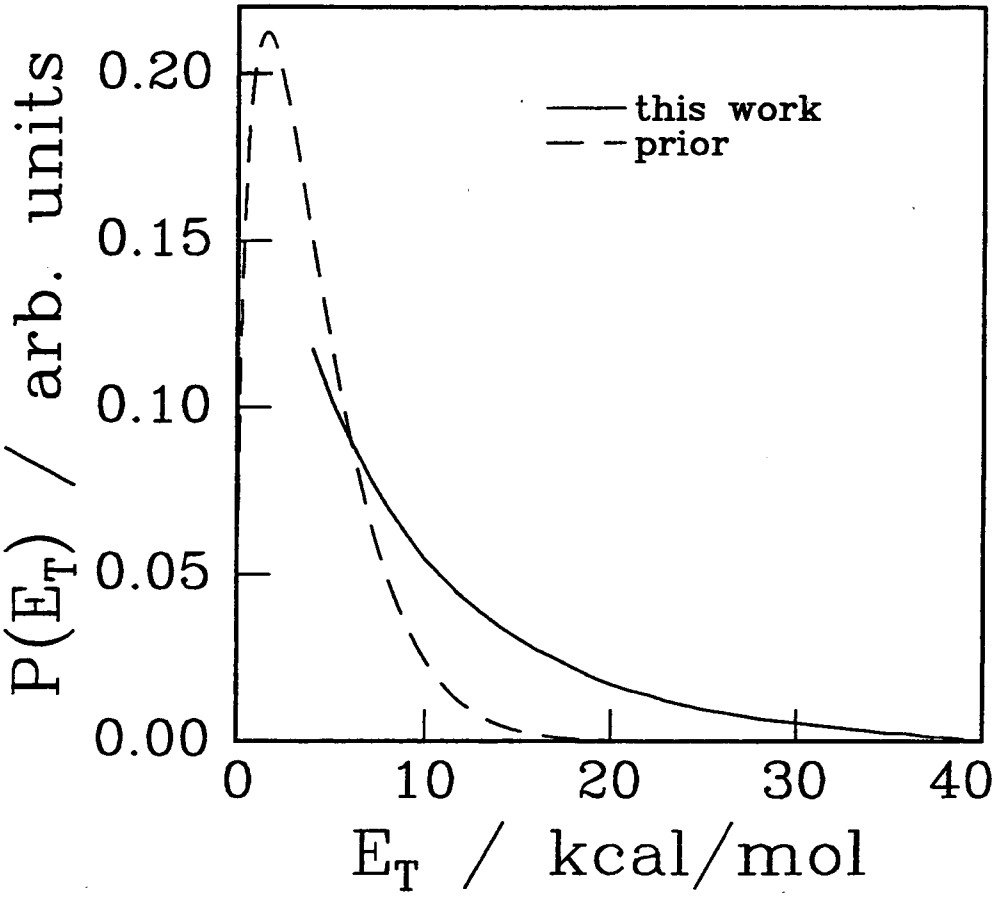
P(E_T) / arb. units
0.20
0.15
0.10
0.05
0.00
0
10
20
30
40
E_T / kcal/mol
this work
prior

figure 3

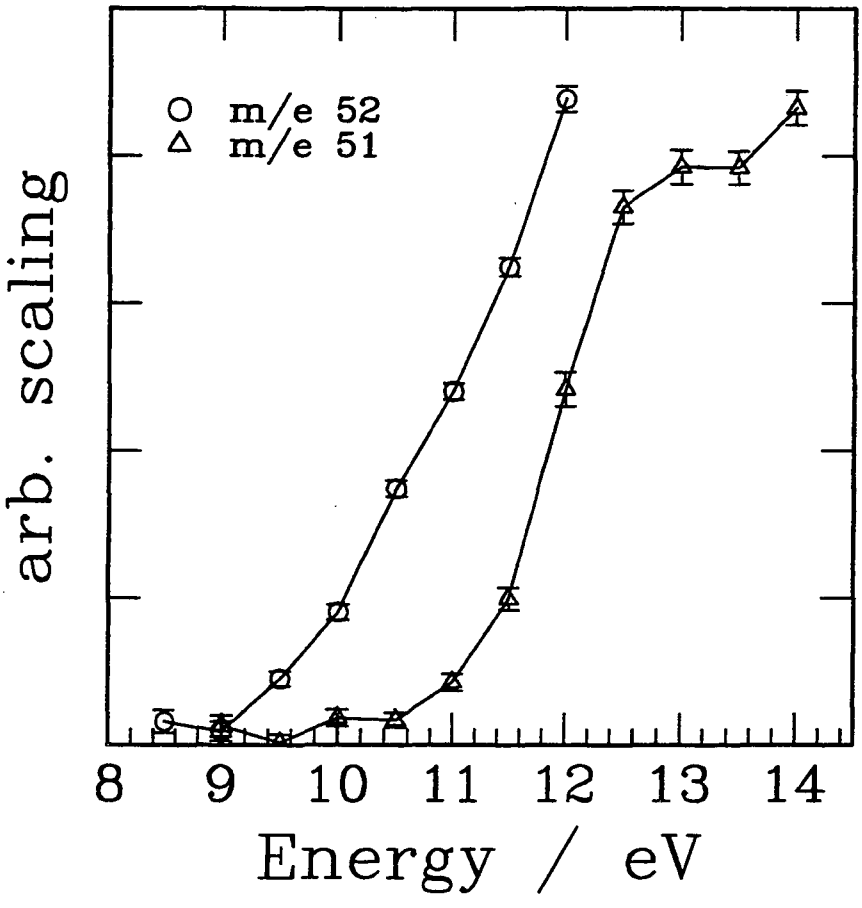

figure 4

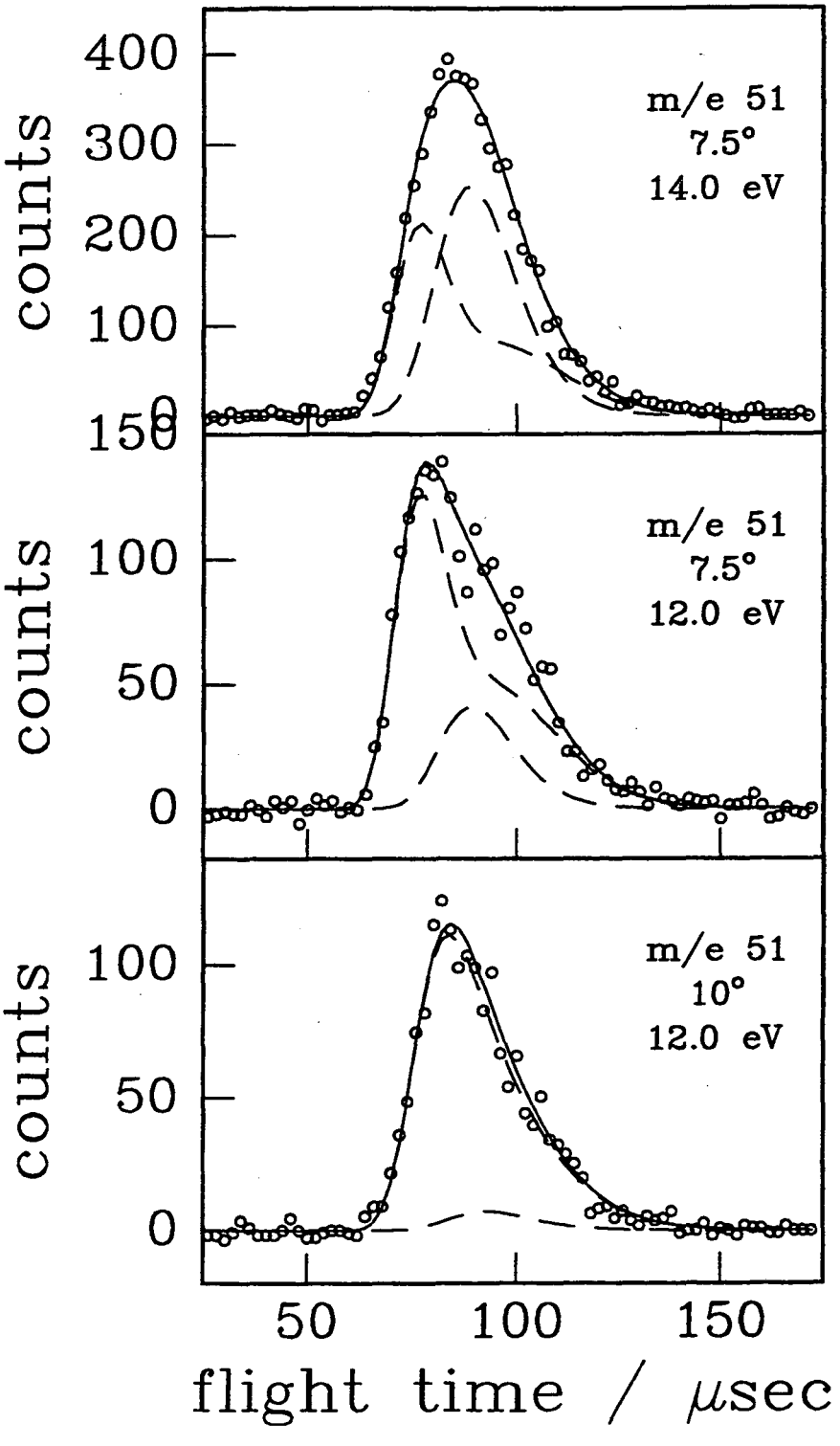
counts
400
300
200
100
0
m/e 51
7.5°
14.0 eV
counts
100
50
0
m/e 51
7.5°
12.0 eV
counts
100
50
0
m/e 51
10°
12.0 eV
50
100
150
flight time / μsec

figure 5

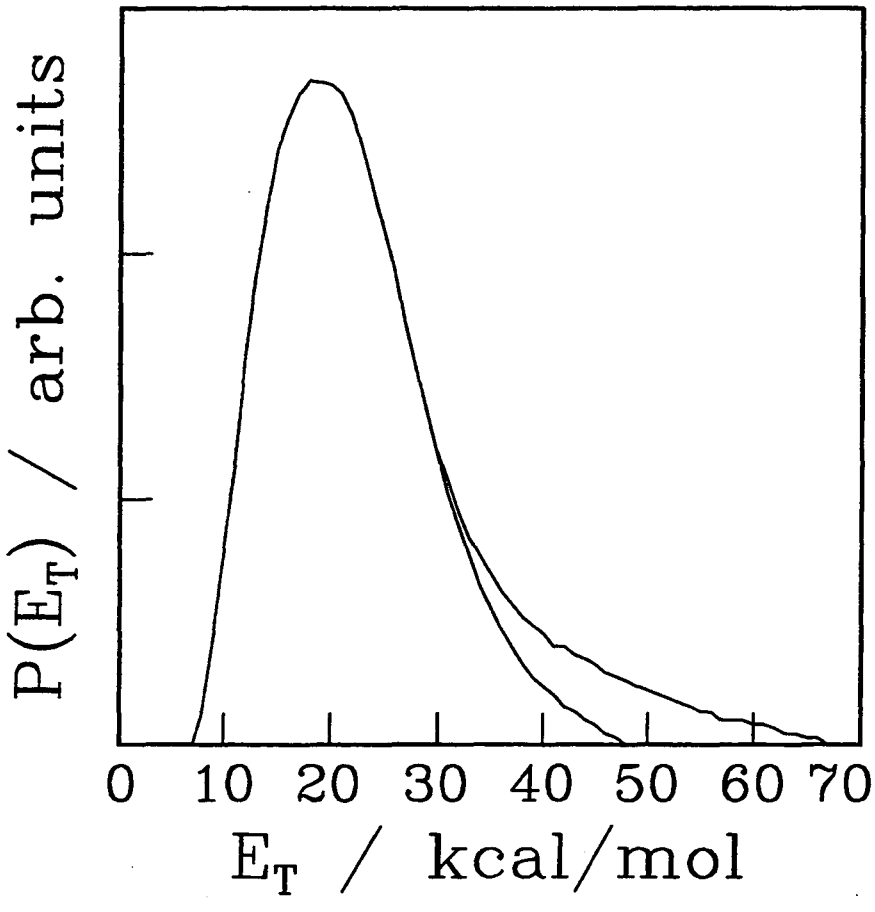

figure 6

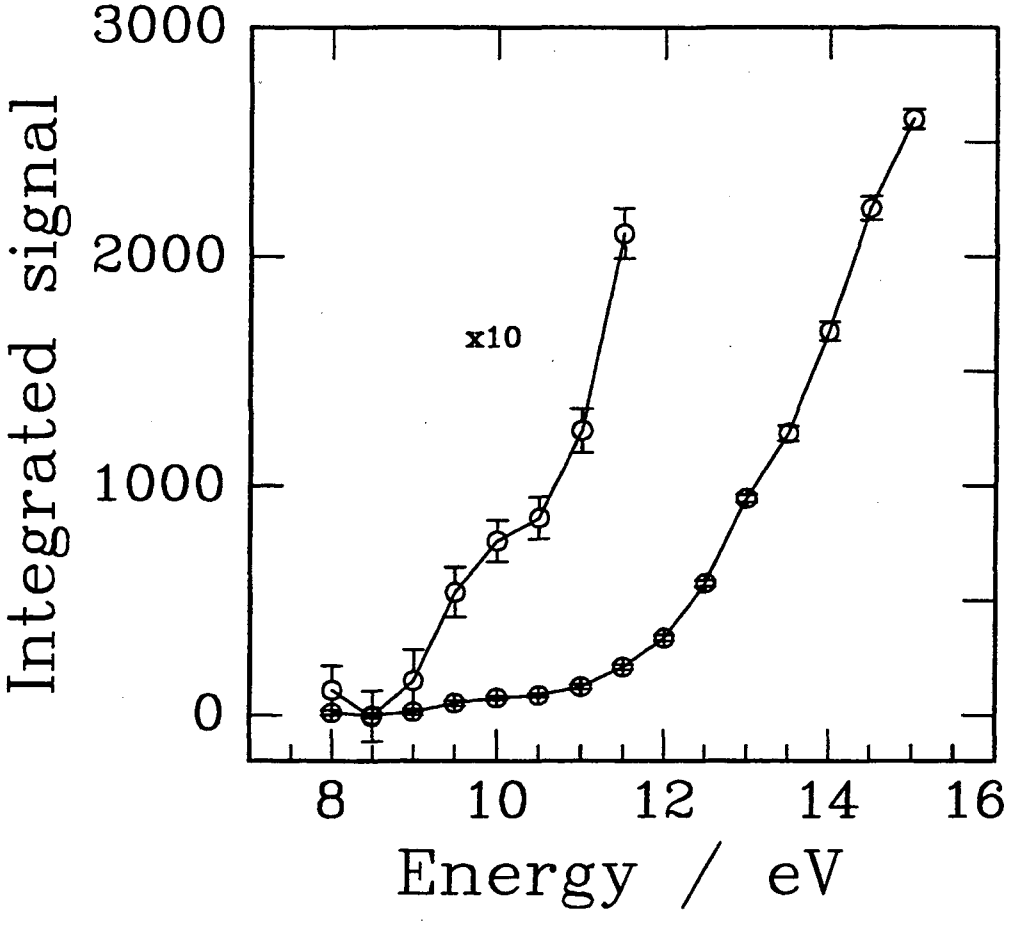

figure 7

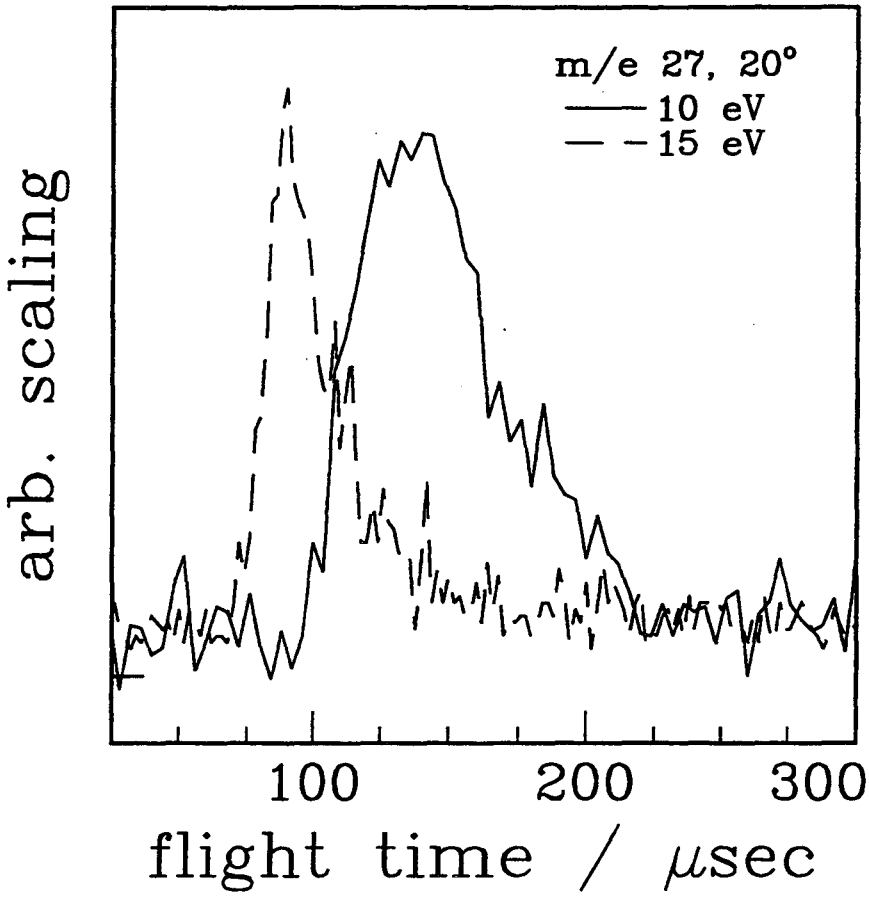

figure 8

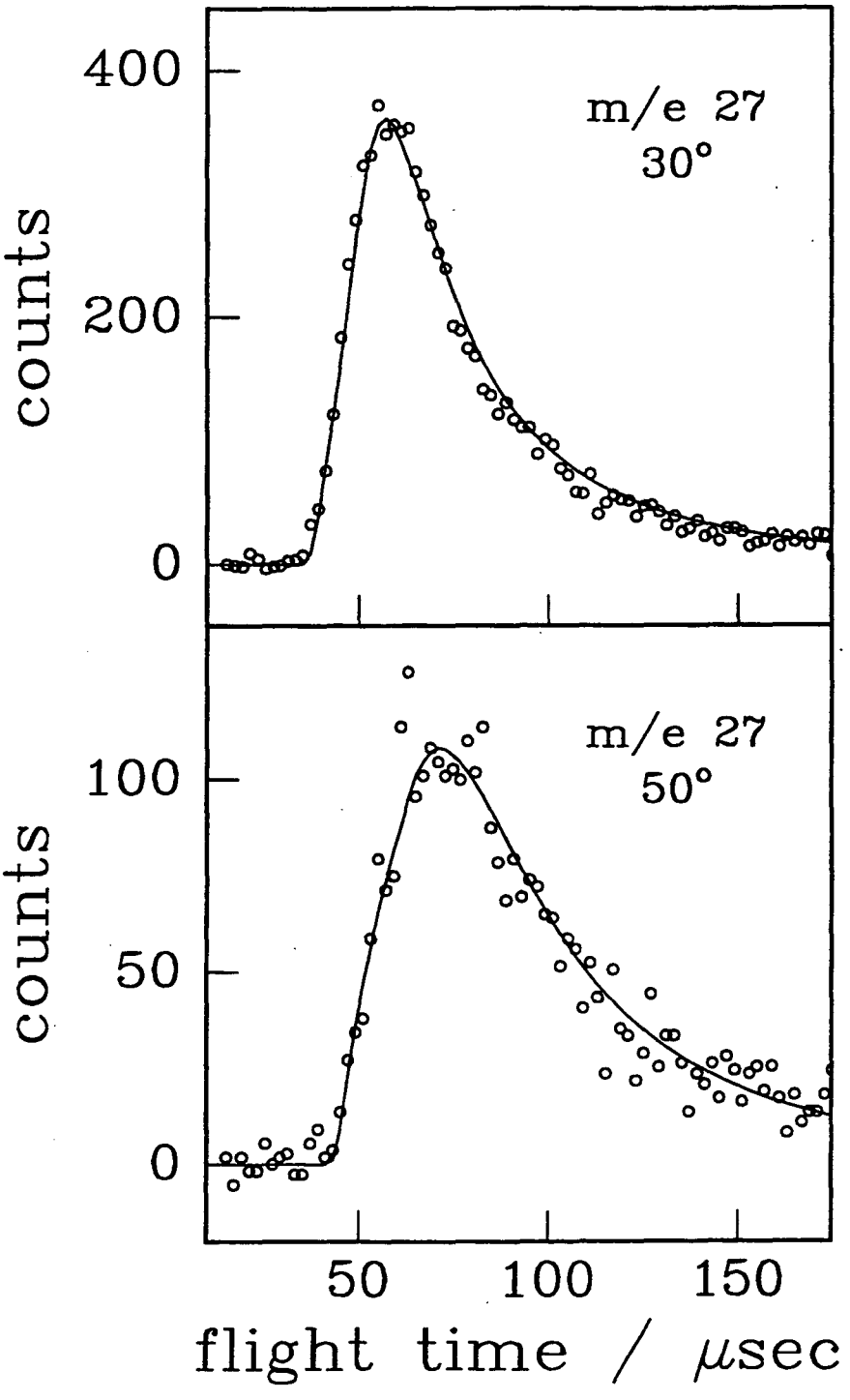
400
200
0
counts
m/e 27
30°
100
50
0
counts
m/e 27
50°
50
100
150
flight time / μsec

figure 9

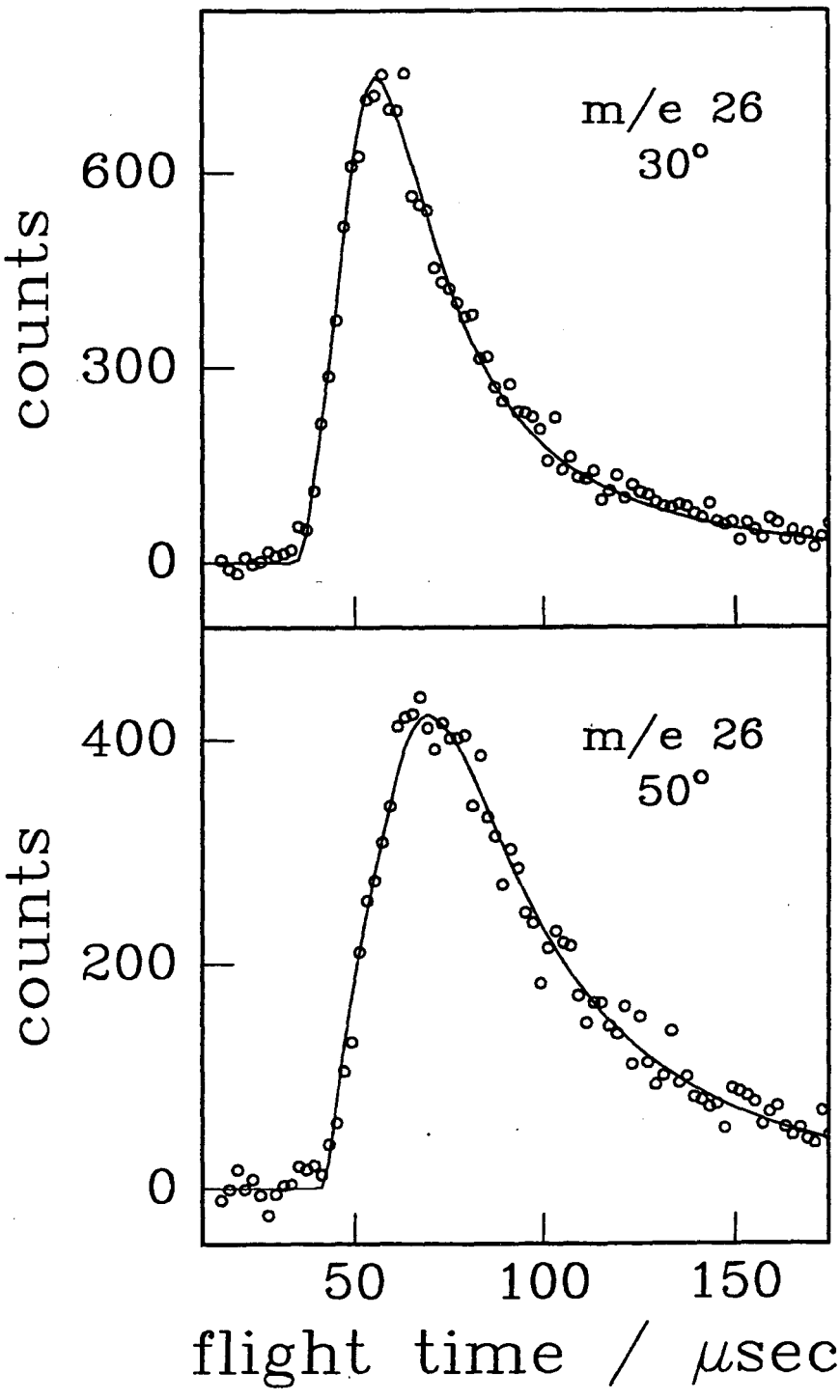
m/e 26
30°
600
300
0
counts
m/e 26
50°
400
200
0
counts
50
100
150
flight time / μsec

figure 10

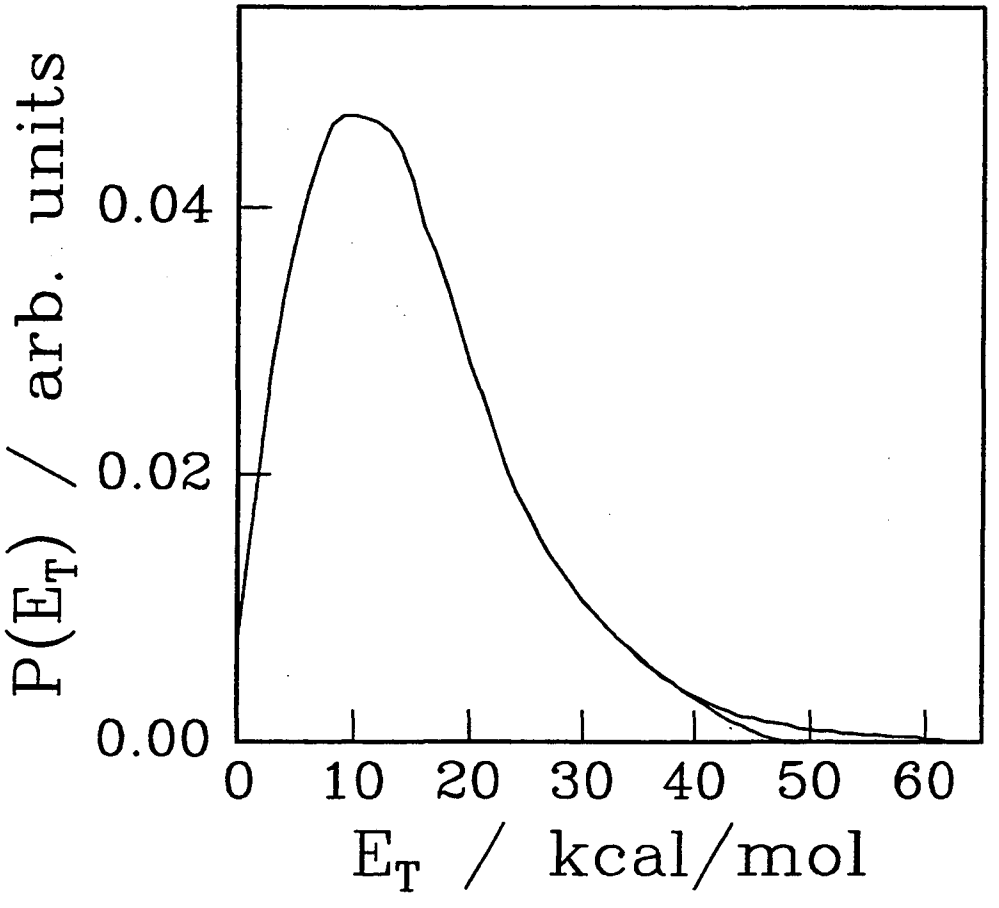

figure 11

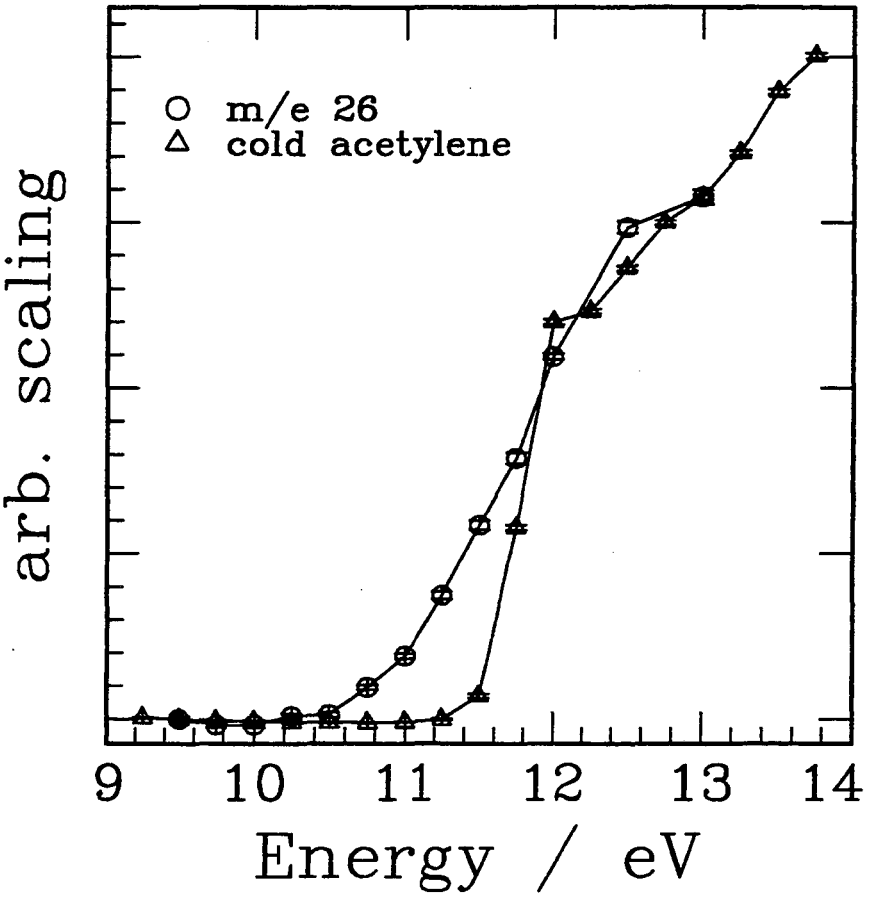

figure 12

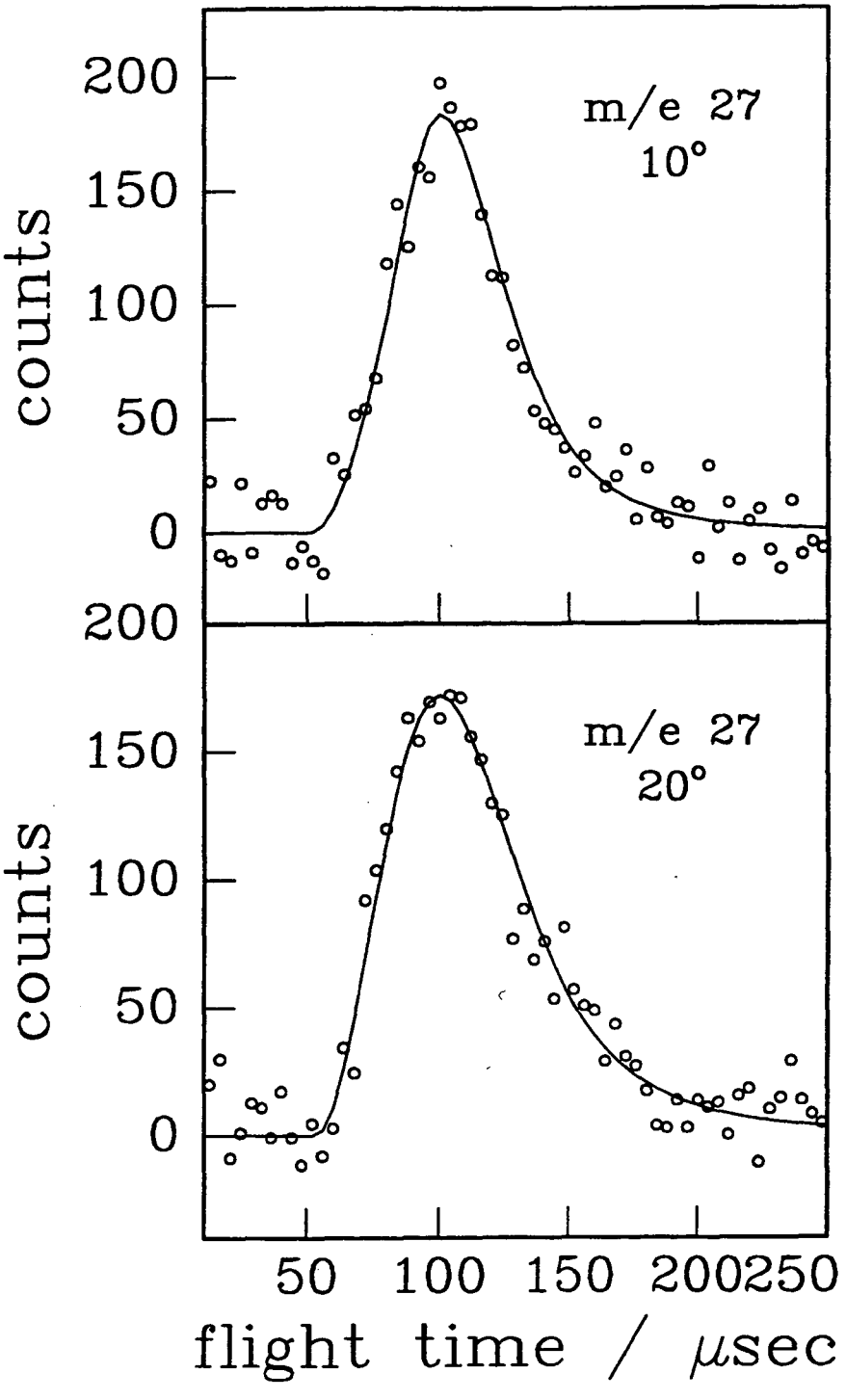
m/e 27
10°
m/e 27
20°
counts
counts
200
150
100
50
0
200
150
100
50
0
50 100 150 200250
flight time / μsec

figure 13

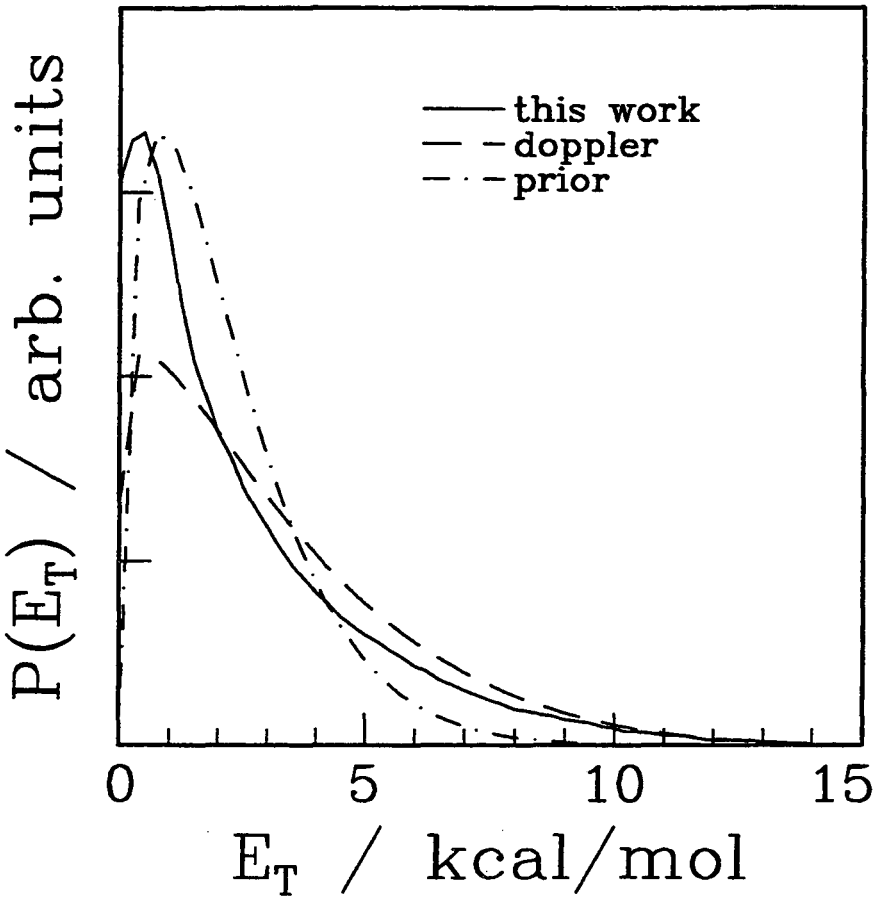

figure 14

ERNEST ORLANDO LAWRENCE BERKELEY NATIONAL LABORATORY
ONE CYCLOTRON ROAD | BERKELEY, CALIFORNIA 94720

Prepared for the U.S. Department of Energy under Contract No. DE-AC03-76SF00098